

compensator more nearly equal to the AR_{\min} of the waveguide run. The AR compensator is found to be an extremely broadbanded device.

CONCLUSIONS

The dominant-mode AR in nominally circular waveguides can easily be obtained from approximate equations, when the difference between the major and minor axes is small and the waveguide is not too long. The calculated values of AR agree quite well with values found by measurements.

The effect of ellipticity on the dominant-mode AR, that is on the amount of crosstalk, is considerable. When waveguide sections are connected in series, the AR of the individual sections can be partially cancelled by properly orienting the sections relative to each other. The orientation of each waveguide section is independ-

ent of the frequency. The amount of cancellation, however, depends on what the values of minimum AR for the various sections are.

The AR performance of a waveguide run can be improved by using an AR compensator. If the minimum AR of the compensator is made about the same as the minimum AR of the run itself and is oriented properly, the total AR will be high for any polarization of the incident dominant-mode signals.

ACKNOWLEDGMENT

The author wishes to thank many associates at the Bell Telephone Laboratories, in particular S. P. Morgan, Jr., for helpful criticism and suggestions in the preparation of this paper. The author is also indebted to those who assisted in making the measurements. Some tests were performed at Western Electric Company.

The Design of Ridged Waveguides

SAMUEL HOPFER†

AS FAR as we are aware, the only published design information on ridged guide transmission lines is found in a paper by S. B. Cohn¹ and to some extent in the Waveguide Handbook.² Recent applications, however, have indicated a need for additional and, in some cases, more accurate design information. The present paper is largely written with this in mind.

The design curves presented here differ in several respects from those found in the literature. The more important differences can be stated as follows:

1. The step discontinuity susceptance is properly included in all calculations. Omission of this effect in calculating the cut-off frequencies of the higher modes, as well as in the calculation of the power carrying capacity, leads to considerable errors.
2. The attenuation calculations are based on a more rigorous expression for ridged guide attenuation.
3. The power handling curves take proper account of the breakdown at the edges.
4. The ridged guide impedance definition is different and seems more in line with experimental results.
5. The data are presented in terms of those parameters most likely to be specified in practice.

† Polytechnic Res. & Dev. Co., Inc., Brooklyn, N. Y.

¹ S. B. Cohn, "Properties of ridge waveguide," *Proc. IRE*, vol. 35, pp. 783-788; August, 1947.

² Nathan Marcuvitz, *Waveguide Handbook*, MIT Rad. Lab. Series, vol. 10, pp. 399-402.

CUTOFF CURVES AS A FUNCTION OF RIDGED GUIDE GEOMETRY

Figs. 1(a) and 1(b) show the single- and double-ridged cross sections; their equivalent circuit representation is shown in Fig. 1(c). In keeping with common practice,

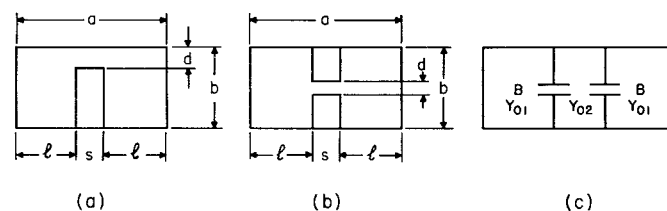


Fig. 1

the ridged guide modes are given the same designations as the corresponding modes in the rectangular waveguide. The equations which govern the cutoff conditions of the TE_{no} type of modes are given by

$$\cot \kappa_x l - \frac{b}{d} \tan \kappa_x s / 2 - B / Y_{01} = 0 \quad (1)$$

$$\cot \kappa_x l + \frac{b}{d} \cot \kappa_x s / 2 - B / Y_{01} = 0. \quad (2)$$

Eq. (1) applies to the odd TE_{no} modes and (2) applies to the even TE_{no} modes. κ_x is the propagation constant in the x direction at cutoff and is given by $\kappa_x = 2\pi/\lambda_c$.

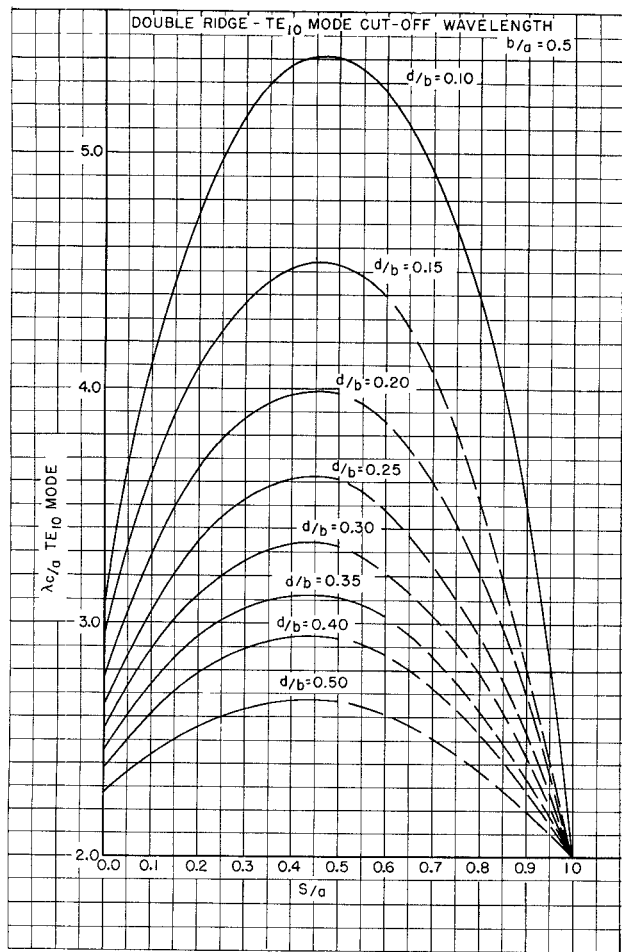


Fig. 2

The characteristic admittances Y_{01} and Y_{02} are defined as

$$Y_{01} = \frac{\kappa_x}{\omega\mu} \frac{1}{b}, \quad Y_{02} = \frac{\kappa_x}{\omega\mu} \frac{1}{d} \quad (3)$$

The value of the normalized susceptance term B/Y_{01} , which represents the effect of the step discontinuity, is taken from published data in the Waveguide Handbook.³ In those cases, where the sidewalls of the guide are relatively close to the step discontinuity of the ridge, proximity effects⁴ are taken into account in the determination of the normalized susceptance B/Y_{01} .

In Figs. 2, 3, and 4 the extension factors λ_{cno}/a for the TE_{10} , TE_{20} , and TE_{30} modes are plotted as a function of s/a , with d/b a parameter. The aspect ratio b/a is fixed at 0.5. These curves are directly applicable to a single ridged guide cross section of identical s/a and d/b ratios, but of an aspect ratio b/a which is one half that of the double ridged guide. Since the electrical properties depend to various degrees upon the ratio

³ Ibid., p. 309.

⁴ J. R. Whinnery, and H. W. Jamieson, "Equivalent circuits for discontinuities in transmission lines," PROC. IRE, vol. 32, pp. 98-116; February, 1944.

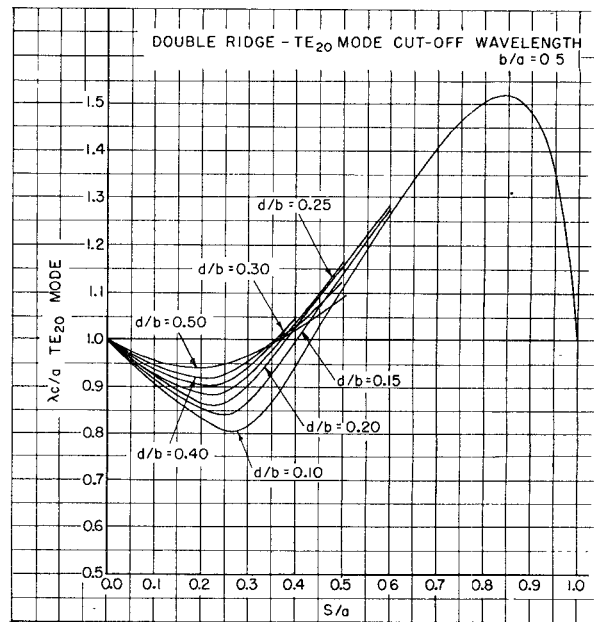


Fig. 3

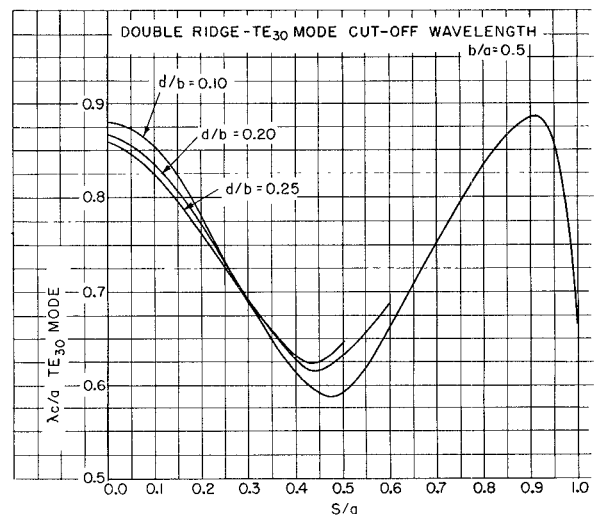


Fig. 4

b/a —and a b/a ratio of 0.25 is not very favorable for the single ridged guide—it is expedient to have single ridged data available for $b/a = 0.45$. These data are in Figs. 5, 6, and 7 (next page). In case of Fig. 7, no values of extension factors for $.08 < (s/a) < .5$ are indicated, because in this range the TE_{30} mode cannot exist by itself but couples to the TE_{01} mode. The extension factors for the fundamental TE_{10} mode at aspect ratios other than 0.45, as in the single ridged guide, may be determined with the help of Fig. 8 (next page). This determination is essentially a first order correction on the value of the extension factor at $b/a = .45$. Expressed in the form of an equation, we have

$$\frac{\lambda_{c10}'}{a} = \frac{\lambda_{c10}}{a} + F_{10} \left(\frac{b}{a} - .45 \right), \quad (4)$$

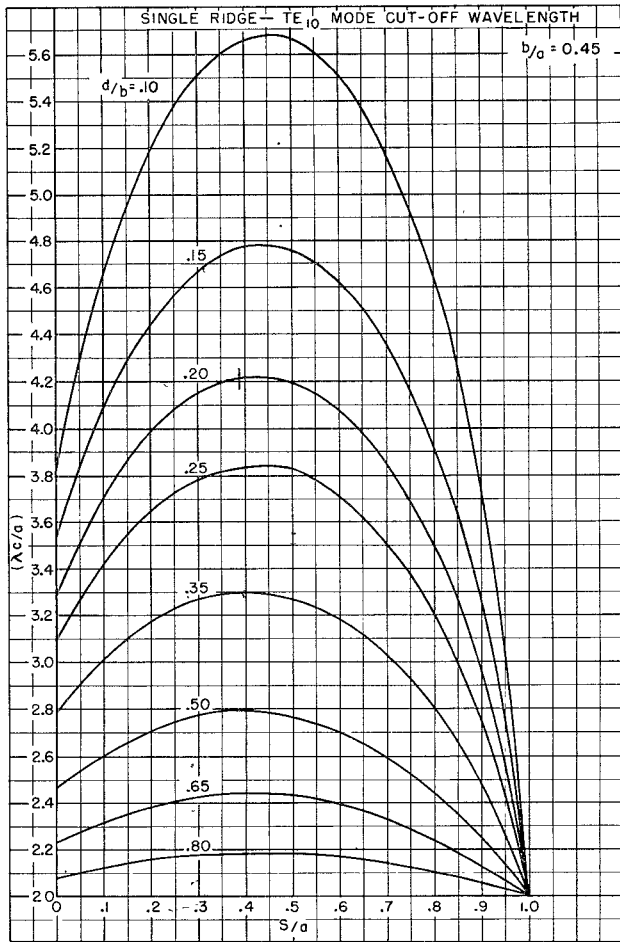


Fig. 5

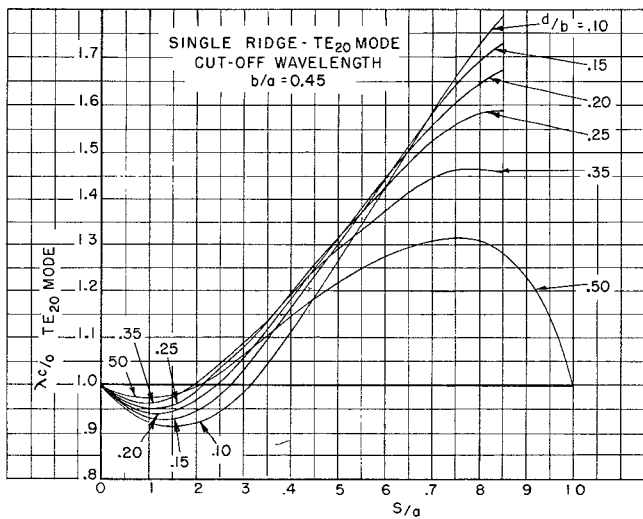


Fig. 6

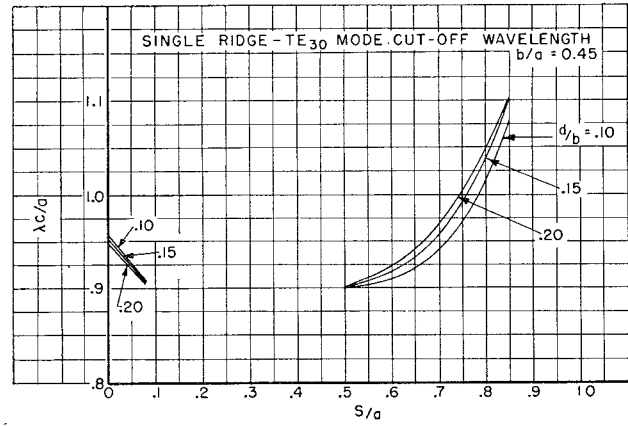


Fig. 7

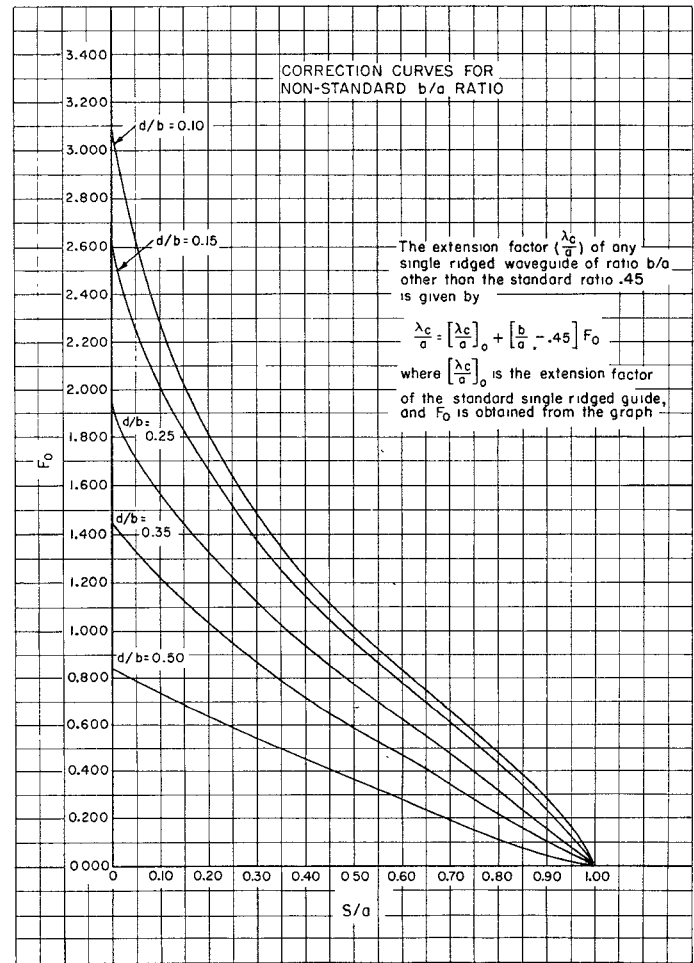


Fig. 8

where λ_{c10}'/a is the desired extension factor at the actual b/a and λ_{c10}/a is the extension factor at $b/a = .45$. The factor F_{10} is a function of the parameters s/a and d/b and is given by

$$F_{10} = \frac{4 \frac{\lambda_{c10}}{a} \ln \csc(\pi d/2b)}{\pi(1 - s/a) \csc^2 \left[\frac{2\pi(1 - s/a)}{\lambda_{c10}/a} \right] + \pi \frac{s/a}{d/b} \sec^2 \frac{\pi s/a}{\lambda_{c10}/a} + 1.8 \ln \csc \frac{\pi d}{2b}} \quad (5)$$

BANDWIDTH CONSIDERATIONS

The term "bandwidth," as used here, is defined as the ratio of the cutoff wavelengths of the fundamental mode and the next higher mode. By inspection of the cutoff

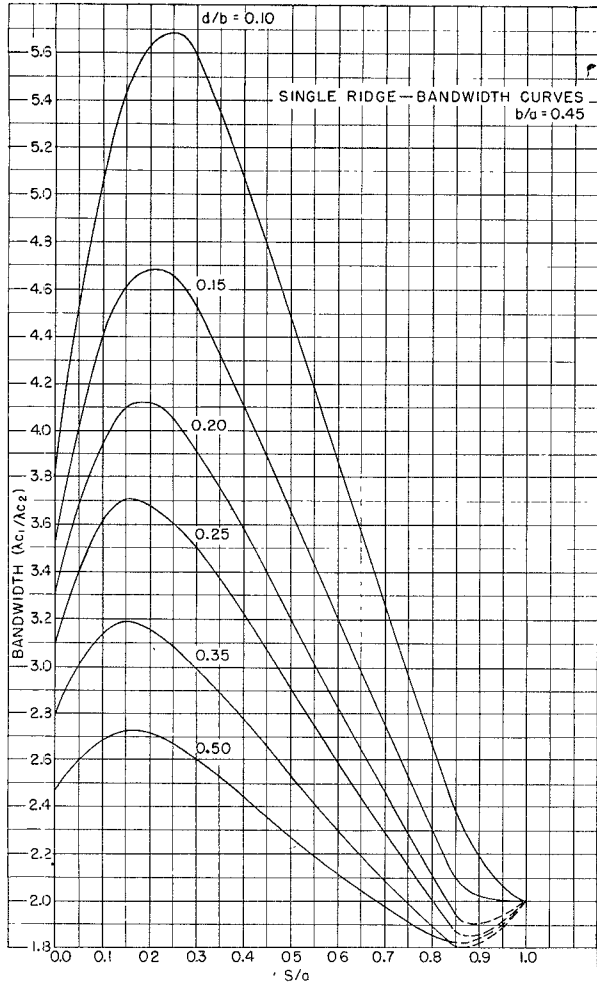


Fig. 9

curves, it is seen that for any given geometry of the ridged guide, the extension factor of the TE_{20} mode is always larger than the corresponding one for the TE_{30} mode. Thus, the cutoff frequency of the third mode is always greater than the cutoff frequency of the second mode. On the other hand, cutoff calculations for the TE_{01} mode show that the cutoff wavelength for this mode is very nearly equal to $2b$. In order to extend the upper bandwidth limit of the ridged guide, to the TE_{20} mode cutoff, the b/a ratio should approximately be made equal to one-half the extension factor of the TE_{20} mode. For large bandwidths, this would require the b/a

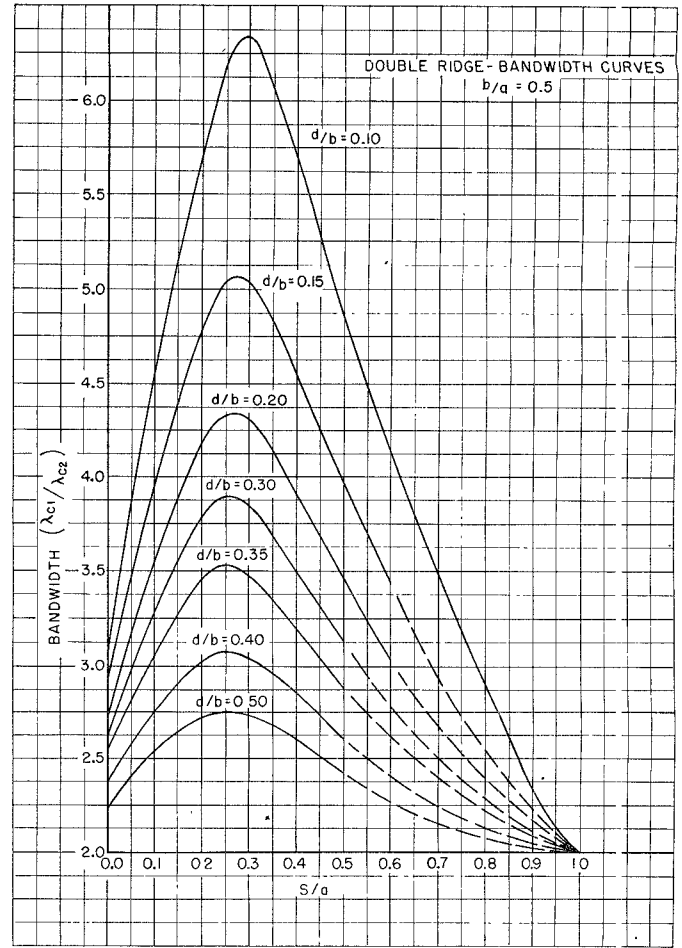


Fig. 10

width" over which the guide may be operated. The latter depends mainly upon how close to the lower cutoff frequency one is willing to work. Experience has shown that this may range anywhere from 15 per cent to 25 per cent above cutoff.

RIDGED GUIDE ATTENUATION

The attenuation σ of the ridged guide transmission line is approximately given by

$$\sigma = 8.686 \frac{\pi \lambda_c / b \lambda^2 + Q}{\sqrt{(\lambda_c / \lambda)^2 - 1}} \rho \text{ db/m} \tag{6}$$

where

$$Q = \frac{\left\{ 2\pi \frac{\alpha - \beta}{\beta^2} \rho^2 \left[\tan \frac{\pi \gamma}{k} + \frac{\pi \gamma}{k} \sec^2 \frac{\pi \gamma}{k} \right] + \frac{4\pi^2}{k} B'^2 \frac{\alpha - \beta}{\alpha} \right\} \tan^2 \frac{2\pi \delta}{k} + \frac{4\pi^2}{k} \sec^2 \frac{2\pi \delta}{k}}{ka^2 \left\{ \frac{2\alpha}{\beta} \left[\tan \frac{\pi \gamma}{k} + \frac{\pi \gamma}{k} \sec^2 \frac{\pi \gamma}{k} \right] \tan^2 \frac{2\pi \delta}{k} - 2 \tan \frac{2\pi \delta}{k} + \frac{4\pi \delta}{k} \sec^2 \frac{2\pi \delta}{k} \right\}}, \tag{7}$$

ratio of the double ridged guide to be about 0.4 and the b/a ratio of the single ridged guide to be about 0.45.

Figs. 9 and 10 show the curves of bandwidth as a function of s/a and d/b for the single- and double-ridged guides, respectively. It should be realized that the "bandwidth" as defined here is not the "useful band-

and where

$$\begin{aligned} \rho &= \text{skin depth in meters} \\ \alpha &= b/a & \gamma &= s/a & k &= \lambda_c/a \\ \beta &= d/a & \delta &= \frac{1 - s/a}{2} & p &= \lambda_c/\lambda. \end{aligned}$$

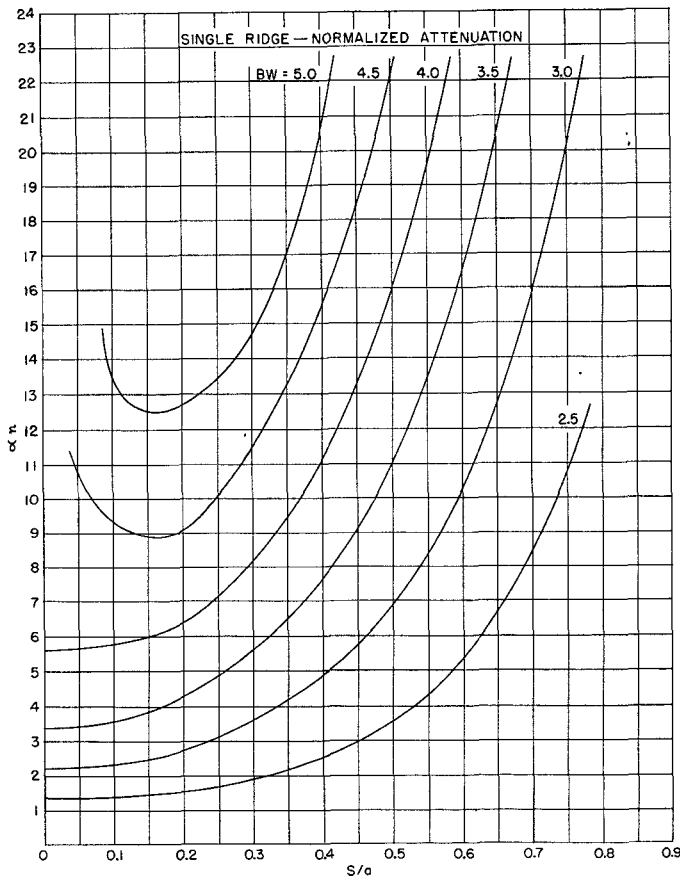


Fig. 11

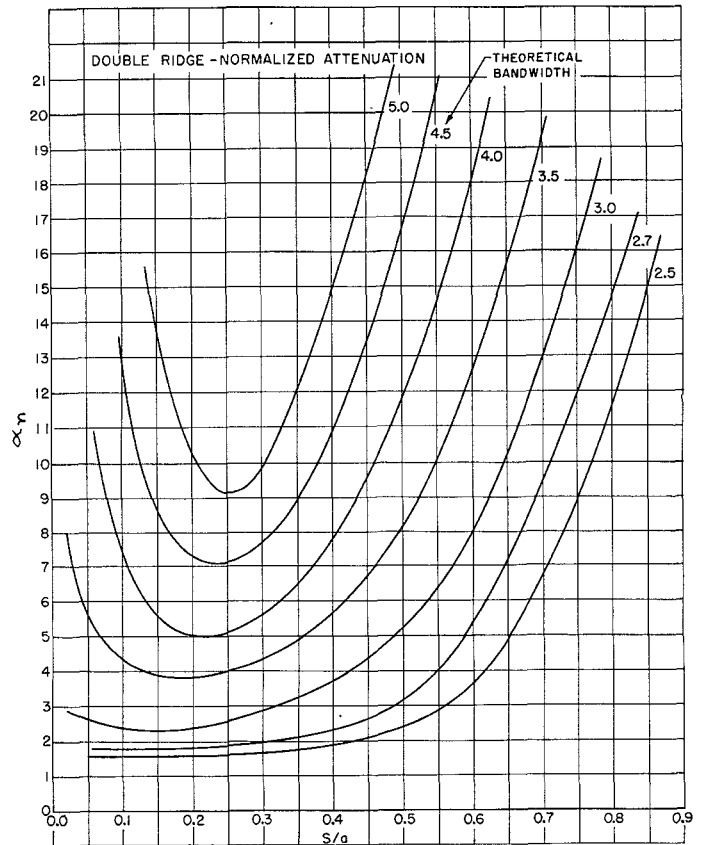


Fig. 12

A derivation of (6) is found in the Appendix. In order to present ridged guide attenuation data in a general fashion, it is convenient to compare the attenuation of the ridged guide to that of a rectangular guide of identical cutoff frequency. We thus define a normalized attenuation σ_n , as the ratio of the ridged guide attenuation to the rectangular guide attenuation of identical cutoff and evaluate this ratio at a frequency $f = \sqrt{3}f_c$. Such curves are shown in Figs. 11 and 12. It can be shown that σ_n increases monotonically, with frequency reaching its average value at about $f = \sqrt{3}f_c$. For bandwidths as large as 5, σ_n does not change by more than ± 25 per cent from the plotted values. In the calculations of the attenuation data it is assumed that the aspect ratio b/a of the rectangular guide is the same as that of the ridged guide. Thus, in the case of the double ridged guide, the normalized attenuation is referred to a rectangular guide of aspect ratio 0.5, and in the case of the single ridged guide to one of aspect ratio 0.45. Actually, most standard waveguides fall within this range. In order to evaluate the actual attenuation of the ridged guide at $f = \sqrt{3}f_c$, σ_n must be multiplied by the rectangular guide attenuation at this frequency. This latter quantity is plotted in Fig. 13 as a function of the guide width, a , for values of $b/a = 0.5$ and $b/a = 0.45$, respectively. It should be noticed, that the value of the ridged guide attenuation, as obtained in the described manner, corresponds very closely to the minimum attenuation over the frequency range, since the latter always occurs in the vicinity of $f = \sqrt{3}f_c$.

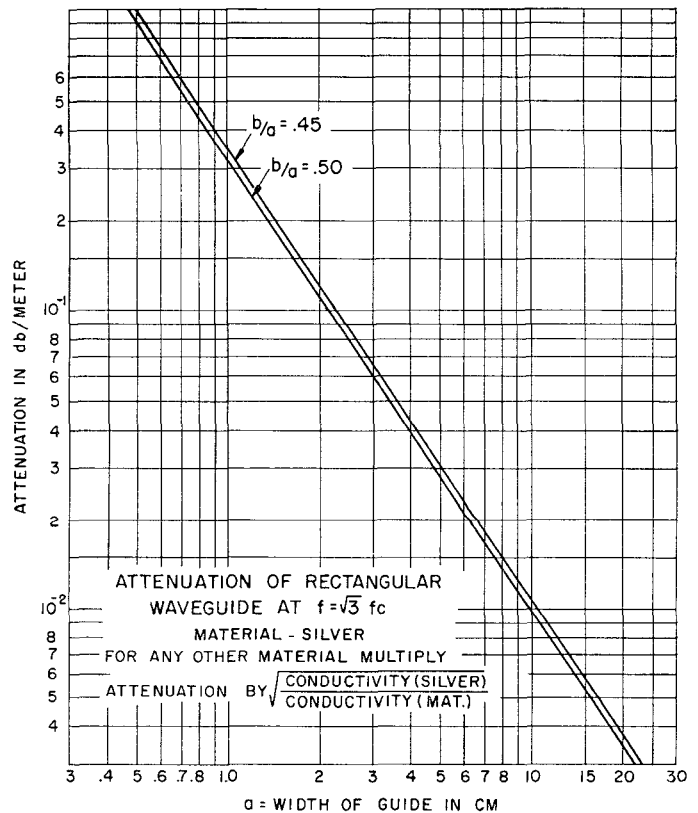


Fig. 13

POWER HANDLING CAPACITY

An approximate expression for the power carried by the ridged guide is given by

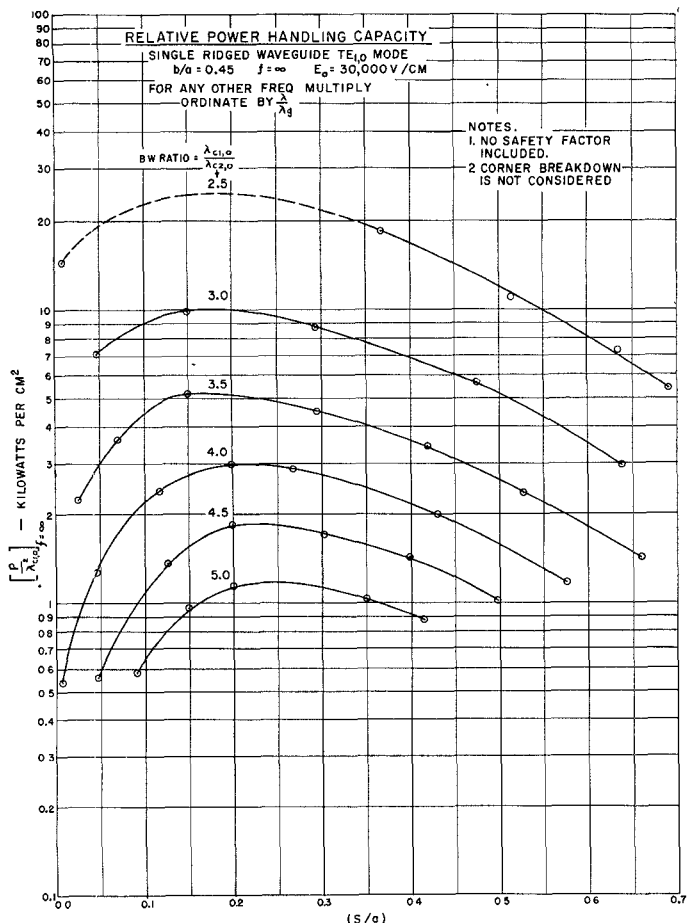


Fig. 14

$$P = \sqrt{\frac{\epsilon_0}{\mu_0}} \frac{\lambda}{\lambda g} \frac{E_0^2}{2\pi} \frac{\beta \lambda_c^2}{k} \left\{ m \frac{2\beta}{k} \cos^2 \frac{\pi\gamma}{k} \ln \csc \frac{\pi d}{2b} + \frac{\pi\gamma}{2k} + \frac{1}{4} \sin \frac{2\pi\gamma}{k} + \frac{d}{b} \frac{\cos^2 \pi\gamma/k}{\sin^2 2\pi\delta/k} \left[\frac{\pi\delta}{k} - \frac{1}{4} \sin \frac{4\pi\delta}{k} \right] \right\} \quad (8)$$

where E_0 is the electric intensity at the center of the ridged gap.

$m = 1$ for the double ridged guide

and

$m = 2$ for the single ridged guide.

A derivation of the above expression is found in the Appendix.

In Fig. 14, the quantity P_m/λ_c^2 is plotted against s/a , with the bandwidth ratio a parameter. P_m represents the power carried by the single ridged guide at infinite frequency, with the electric intensity E_0 at the center of the guide being equal to 30 kv per cm. P_m is thus seen to represent the maximum power which could possibly be handled by the ridged guide, if an air dielectric at standard conditions is assumed. In order to achieve this value for the maximum power handling ability, it would be necessary that the breakdown occurs at the center of the ridged guide. This, however, is generally not the case, because the electric intensity at the edges of the ridge is normally higher than at the center. In view of the critical dependence of the electric intensity on the roundness of the edge, it is convenient to relate E_s ,

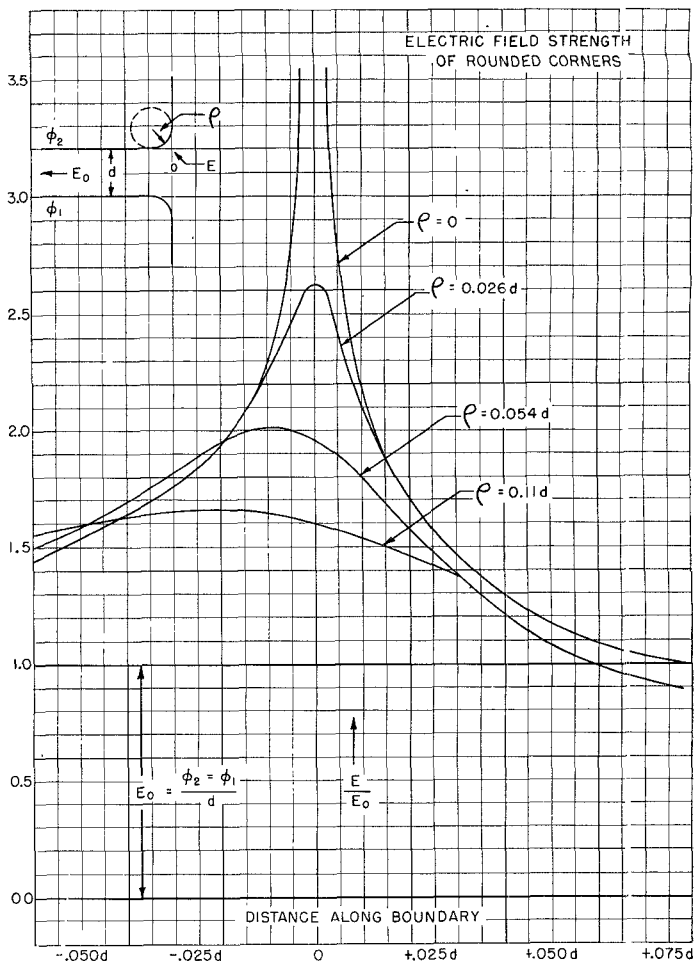


Fig. 15

the electric intensity in the vicinity of the edge to E_0 the electric intensity at the center, as a function of the radius of curvature of the edge. This is shown in Fig. 15 in which the ratio E_s/E_0 is plotted as a function of the edge coordinate, with the radius of curvature a parameter. The curves of Fig. 15 apply to the static case of a corner above a grounded plane. This case is treated in the literature.⁵ Due to the variation of the electric intensity in the ridged gap, the E_s/E_0 ratio, as found from the curves in Fig. 15, is always higher than in the actual dynamic case. An approximate expression for E_s/E_0 dynamic is given by

$$(E_s/E_0) \text{ dyn.} = \cos. \frac{\pi s}{\lambda c} \left(\frac{E_s}{E_0} \right) \text{ stat.} \quad (9)$$

It should be evident that the curves in Fig. 15 are only applicable if ρ is very much smaller than any one of the physical dimensions of the ridged cross section. In the calculation of the maximum power handling capacity of a ridged guide, it is thus necessary to ascertain first value of E_s/E_0 dyn. If the latter is less than unity, then the curves of Fig. 14 may be used directly, however, if E_s/E_0 dyn. is larger than unity, then the value obtained from Fig. 14 must be divided by (E_s/E_0) dyn.⁶

⁵ R. Rothe, F. Ollendorf, and K. Pohlhausen, "Theory of Functions as Applied to Engineering Problems," Murray Printing Co., pp. 129-136; 1942.

⁶ Marcuvitz, op. cit.

RIDGED GUIDE IMPEDANCE

In order to design transitions between the ridged waveguide and a coaxial line or between any two dissimilar waveguides, one is forced to compare the impedances of the two guides. Although the value of impedance designations in this connection is highly questionable, it is, nevertheless, very useful in many instances as shown in the section on special applications. The impedance definition adopted for the calculation of the ridged guide impedance is

$$Z_0 = V_0^2/2P,$$

where V_0 is the peak voltage across the center of the ridge, and where P represents the average power carried by the guide. For convenience, the admittance rather than the impedance is plotted in Fig. 16, as a function of the ridged guide geometry. The admittance values shown apply to infinite frequency and must therefore be multiplied by the factor λ/λ_0 , in order to yield the correct value at any given frequency.

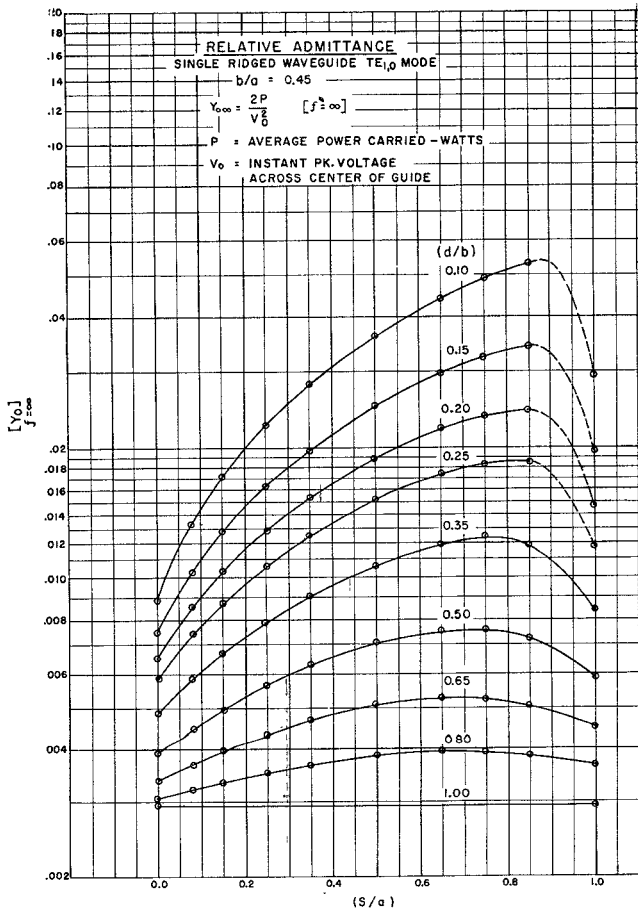


Fig. 16

SPECIAL APPLICATIONS

While the large bandwidths obtainable with ridged guide favor its use as a system by itself, nevertheless, ridged guide sections are frequently used in conjunction with the standard rectangular guides. Invariably, such

applications involve transitions from ridged to rectangular waveguide. While tapered ridges could be used for this purpose, it is more efficient and probably less costly to employ several quarter-wave ridged sections to effect the transition. The various ridged sections may be arranged in such a manner that the standing wave ratio over the frequency band has a nearly Tchebycheff behavior. If we refer to the symbols used in Fig. 17, we see that the basic design formula for the stepped transition is given by

$$\alpha_i \ln Z_i' = \ln Z_i, \tag{11}$$

where

$$Z_i' = \frac{Z_{i-1}}{Z_i}, \quad Z_1' = \frac{Z_{in}}{Z_1}, \quad Z_N' = \frac{Z_{N-1}}{Z_{out}}$$

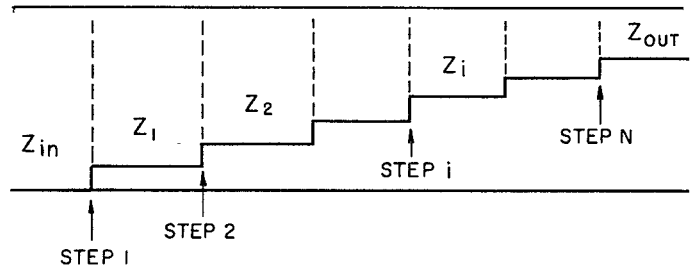


Fig. 17

Eq. (11) is readily solved for Z_1' in terms of the impedance transformation ratio Z_{in}/Z_{out}' which is normally specified; thus

$$Z_1' = \left(\frac{Z_{in}}{Z_{out}} \right)^{1/\sum_1^N \alpha_i} \tag{12}$$

Once Z_1' is determined by (12), all successive impedances are given by

$$Z_i = Z_{i-1}(Z_1')^{-\alpha_i}.$$

TABLE I

| N | a_1 | a_2 | a_3 | a_4 | a_5 | a_6 | a_7 | $\sum_1^N \alpha_i$ |
|-----|-------|-------|-------|-------|-------|-------|-------|---------------------|
| 2 | 1 | 1 | | | | | | 2 |
| 3 | 1 | 1.41 | 1 | | | | | 3.41 |
| 4 | 1 | 2.12 | 2.12 | 1 | | | | 6.24 |
| 5 | 1 | 2.83 | 3.83 | 2.83 | 1 | | | 11.49 |
| 6 | 1 | 3.53 | 6.03 | 6.03 | 3.53 | 1 | | 21.12 |
| 7 | 1 | 4.24 | 8.73 | 10.94 | 8.73 | 4.24 | 1 | 38.88 |

The α_i 's in Table 1, above, are computed to cover the normal bandwidth of the standard rectangular guide; i.e., the ratio of the λ_g 's corresponding to the lowest and highest frequency at which the rectangular waveguide is operated is assumed to be 2.143. They are not optimum when a smaller bandwidth is to be covered. Fig. 18 shows a plot of (12) for a varying number of steps used in each transition. In specifying the input and output impedance, it was found experimentally that by using the $Z_{0\infty}$ values of the respective guides,

better over-all results are obtained than by specifying the characteristic impedance at the center frequency of the design. The values for a given ridged guide geometry, including the rectangular guide are directly obtained from Fig. 16. Having determined the $Z_{0\infty}$'s of the various sections, we again employ Fig. 16 to obtain the necessary ridged guide geometry to yield the desired $Z_{0\infty}$.

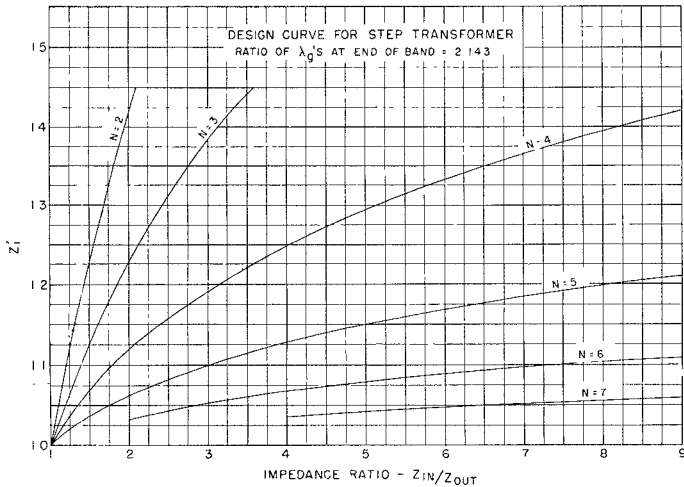


Fig. 18

From a standpoint of easy fabrication, it is desirable to keep the dimension s , the width of the ridge, constant throughout. The length of each transformer section is given by

$$l = \frac{\lambda_{g1}\lambda_{g2}}{2(\lambda_{g1} + \lambda_{g2})} \quad (13)$$

where λ_{g1} , and λ_{g2} are the guide wavelengths of the respective section at the two ends of the frequency band. The λ_g 's for each section are determined with the aid of Fig. 5. In general, therefore, the length of each section will be different. The theory underlying the transformer design is based on many simplifying assumptions which make difficult the accurate prediction of the vswr response for a given number of sections. It has been found experimentally that 4 section transformers designed in accordance with the above design formulas will cover the entire waveguide band with a maximum vswr between 1.15–1.20 for $Z_{0\infty}$ transformation ratios of as high as 4.3.

APPENDIX

ATTENUATION CALCULATION

Rather than to attempt to find the approximate field distribution in the ridged guide and to determine from it the current distribution in the walls of the guide, the following derivation is presented in outline and is entirely based on transmission line calculations. This method was suggested to the author by Dr. N. Marcovitz.

We start with the well-known relation between the variously directed periodicities in a uniform guided system:

$$K^2 = \kappa_z^2 + \kappa_{cx}^2 + \kappa_{cy}^2 \quad (14)$$

where

$$K^2 = \omega^2/\mu\epsilon$$

$$\kappa_z = \beta - j\sigma$$

$$\beta = 2\pi/\lambda_g$$

σ = attenuation constant in nepers per meter.

κ_{cx} and κ_{cy} are wave numbers due to resonances in the x and y directions. If the dielectric in the guide is lossless, then K^2 is real and consequently κ_{cx} and κ_{cy} must be complex if κ_z is complex. Consider Fig. 19. The

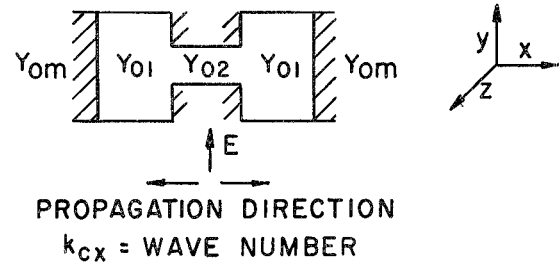


Fig. 19

value of κ_z for propagation along the guide must be the same for both regions 1 and 2. Since K is also the same throughout the cross-section it follows that

$$\kappa_{cx1}^2 + \kappa_{cy1}^2 = \kappa_{cx2}^2 + \kappa_{cy2}^2. \quad (15)$$

In order to determine κ_{cy1} and κ_{cy2} , we assume an E wave to propagate in the y direction and being reflected by the slightly lossy top and bottom walls, as shown in Fig. 20. The metallic medium has a complex phase

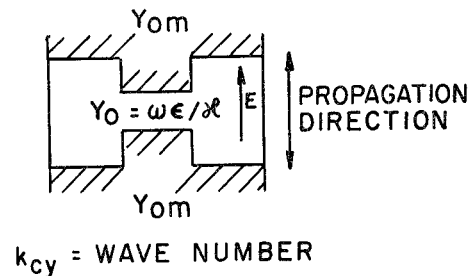


Fig. 20

constant $\kappa_{om} = (1-j)/\rho$ and a complex characteristic admittance $y_{om} = K_{om}/\omega\mu$, where ρ is the skin depth. The characteristic admittance Y_{01} , Y_{02} of the medium between the parallel plates is $\omega\epsilon/\kappa_{cy}$ for an E wave. At $y=b/2$ the admittance is infinite, since the nonvanishing tangential E at the top and bottom walls must reverse itself. The input admittance for medium 1 at $y=b/2$ is thus given by

$$Y_{in} = Y_{01} \frac{j + \frac{Y_{om}}{Y_{01}} \cot \kappa_{cy} b/2}{\cot \kappa_{cy} b/2 + j \frac{Y_{om}}{Y_{01}}} \quad (16)$$

In view of the smallness of κ_{cy1} , the above equation leads to

$$\kappa_{cy1}^2 = -(1-j)K^2\rho/b, \quad (17)$$

and similarly for medium 2

$$\kappa_{cy2}^2 = -(1-j)K^2\rho/d. \quad (18)$$

To determine the wave numbers κ_{cx1} and κ_{cx2} , consider the equivalent circuit of Fig. 21. The step discontinuity is now represented by a shunt impedance, which is composed of two parts; the capacitive reactance, and, in series with it, the impedance of the wall forming the step. The former is assumed to be unaffected by the wall losses, and the latter is assumed to be given by $\omega\mu\rho(b-d)/(1-j)$. The total shunt admittance is thus represented by

$$Y_s = \frac{1}{\omega\mu\rho(b-d)/(1-j) - j/B} \\ \simeq \frac{B^2\omega\mu\rho(b-d)}{2} + jB.$$

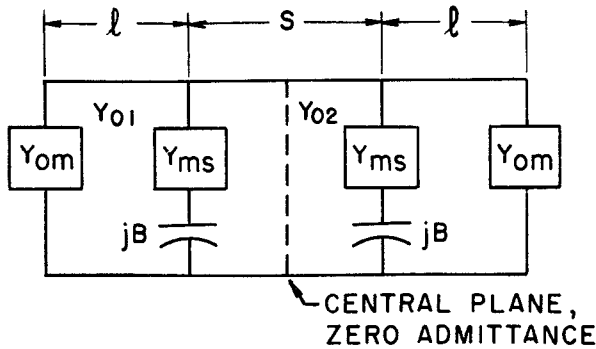


Fig. 21

The condition of transverse resonance in the X direction is satisfied if

$$(Y_{om}) \text{ transformed} + (Y_c) \text{ transformed} + Y_s = 0, \quad (19)$$

where for convenience all admittances are transformed to the plane of the step. Y_c is the zero admittance existing at the central plans. Eq. (19) contains both κ_{cx1} and κ_{cx2} , however, one of these quantities can be eliminated by using (15), (17) and (18). If we take into account the following conditions for small losses

$$\begin{aligned} \text{Re}(\kappa_{cx1}) &\gg \text{Im}(\kappa_{cx1}) \\ \text{Re}(\kappa_{cx2}) &\gg \text{Im}(\kappa_{cx2}) \\ \text{Re}(\kappa_{cx1}) &\gg \text{Re}(\kappa_{cy1}) \\ \text{Re}(\kappa_{cx2}) &\gg \text{Re}(\kappa_{cy2}) \end{aligned}$$

and ignoring all second order quantities, a complex solution for κ_{cx} is obtained. Finally, the attenuation constant is obtained from the relationship

$$\begin{aligned} \kappa_z^2 &= (\beta - j\sigma)^2 = \kappa^2 - \kappa_{cx1}^2 - \kappa_{cy1}^2 \\ &= \kappa^2 - \kappa_{cx2}^2 - \kappa_{cy2}^2 \end{aligned}$$

to yield the expression in the text, namely

$$\sigma = \frac{\pi\lambda_c/b\lambda^2 + Q}{\sqrt{(\lambda_c/\lambda)^2 - 1}} \rho.$$

POWER HANDLING CALCULATIONS

Again consider the situation at cutoff. The total field in the cross-section is a superposition of the fundamental TEM mode at cutoff and all the higher E modes set up by the step discontinuity. We shall now treat the fundamental mode distribution by assuming that the total field at the center of the ridge is that of the fundamental mode. From transmission line theory the voltage distribution is given by

$$V_{(x)} = V_{(0)} \cos \kappa x - jZI_{(0)} \sin \kappa x.$$

Thus, when $V_{(0)}$ is the voltage at the center of the ridge, the voltage distribution in the ridged part of the cross section is given by

$$V_{(x)} = V_{(0)} \cos \kappa x \quad 0 \leq x \leq s/2$$

since

$$I_{(0)} = 0$$

and similarly for the unridged part

$$V_{(x')} = -jZI_{(0')} \sin \kappa x' \quad 0 \leq x' \leq l$$

where we have chosen the origin ($0'$) at the side wall of the guide. At $x = s/2$ corresponding to $x' = l$, the two voltages must be continuous since the effect of the step is purely shunt. This leads to

$$E(x) = E_{(0)} \cos \frac{2\pi}{\lambda_c} x \quad 0 < x < s/2$$

$$E(x') = \frac{d}{b} E_{(0)} \frac{\cos 2\pi/\lambda_c s/2}{\sin 2\pi/\lambda_{cl}} \sin \frac{2\pi x'}{\lambda_c} \quad 0' \leq x' \leq l.$$

Now consider a differential volume element as shown in Fig. 22.

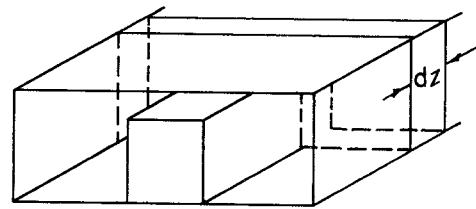


Fig. 22

The maximum electric energy contained in the fundamental mode in the volume element $A dz$ is given by

$$dU_1 = \left[\int_A \int \frac{1}{2} \epsilon_0 E^2 dA \right] dz.$$

The above value is also equal to the total energy in the fundamental mode at any time. The energy contained in the fringing field is approximated by

$$dU_2 = \frac{1}{2} CV^2 dz,$$

where V is assumed to be the first mode voltage at the

step and C is approximately expressed by

$$C \sim \frac{2\epsilon_0}{\pi} \ln \csc(\pi d/2b) \text{ farads/meter.}$$

The total energy in the volume element becomes

$$dU_T = \left[\int_A \int \frac{1}{2} \epsilon_0 E^2 dA + CV^2 \right] dz,$$

and the power in the z direction is given by

$$\frac{dU_T}{dt} = \left[\int_A \int \frac{1}{2} \epsilon_0 E^2 dA + CV^2 \right] \frac{dz}{dt},$$

where dz/dt is the group velocity which is given by $(1/\sqrt{\epsilon_0\mu_0})\lambda/\lambda_g$. Evaluation of the last expression yields (8) of the text.

ACKNOWLEDGMENT

The major part of the work reported in this paper was sponsored by the Bureau of Ships under Contract No. NObsr-39294 and by the Signal Corps under Contract No. DA36-039-sc-42662. It was carried out by the following people of the Polytechnic Research & Development Co., Inc. staff: W. E. Waller, M. Sucher, S. Rubin, L. Kent, C. Kossmann, and the author.

Shielded Coupled-Strip Transmission Line

S. B. COHN†

Summary—An analysis is made of the odd and even TEM modes on a pair of parallel co-planar strips midway between ground planes. Rigorous formulas are presented for the case of zero-thickness strips, while approximate formulas are given for strips of finite thickness and for strips printed on opposite sides of a thin dielectric sheet supported in air between ground planes (AIL construction). The characteristic impedances and the phase velocities of the two modes are necessary and sufficient information for the design of directional couplers, coupled-line filters, and other components utilizing the coupling between parallel-strip lines. In order to facilitate design work, nomograms are included in the paper which give the dimensions of the coupled-strip cross section in terms of the odd- and even-mode characteristic impedances. The characteristic-impedance scales of these nomograms may be read to an accuracy of better than one per cent over a wide range of values that is sufficient for most purposes.

INTRODUCTION

NUMEROUS strip-line components utilize the coupling between parallel strips as a basic parameter in their design. Several examples of such components are shown in Fig. 1 (next page), where coupled lines are used to achieve a particular effect in each case. In order to design these circuits to meet prescribed performance specifications, it is necessary to have accurate data on the coupling effects of parallel strips. Solutions for the most important parameters have been obtained, and are presented in this paper.

Fig. 2 (next page) shows transverse field distributions for two fundamental TEM modes that can exist on a pair of parallel conducting strips between parallel ground planes. In Fig. 2(a), strips are at same potential and carry equal currents in the same direction. Because of the even symmetry of the electric field about the vertical axis, this mode will be called the *even* coupled-strip mode. In Fig. 2(b), strips are at equal but opposite potentials and carry equal currents in opposite directions.

Due to the odd symmetry of the electric field, this mode will be called the *odd* coupled-strip mode. In the case of the odd mode, the vertical plane of symmetry is at ground potential, and may be replaced by a thin conducting wall joined electrically to the horizontal ground plates. It is clear from the field plots that the capacitance per strip to ground is less for the even case

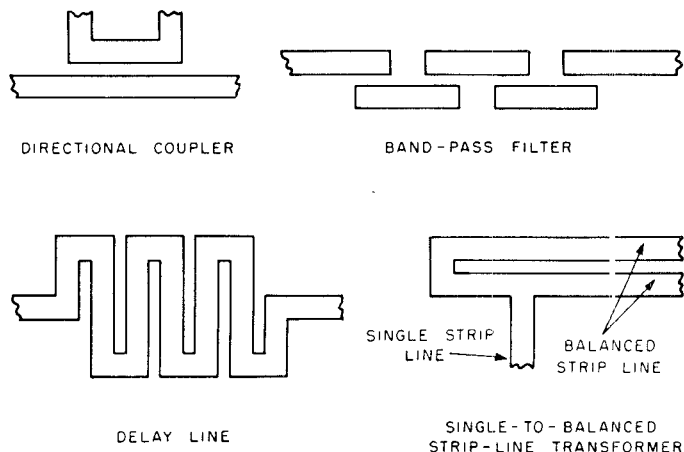


Fig. 1—Several applications of coupled-strip line construction.

and more for the odd case than for a single isolated strip of the same width. Consequently, the characteristic impedances of the two modes are unequal, being greater for the even than for the odd. In this paper, solutions for the two characteristic impedances will be given.¹ These quantities (plus the mode phase velocities, which are also treated) provide sufficient information for the

¹ (After this paper was prepared, a paper by D. Park appeared with a solution for Z_0 of the odd mode. The use of elliptic-integral identities shows Park's formula to be the same as mine.) D. Park, "Planar transmission lines," TRANS. IRE, vol. MTT-3, pp. 8-12; April, 1955.

† Stanford Res. Inst., Menlo Park, Calif.